

Experimental Study on Flow and Mass Transfer in Rotor-Stator Disk Cavities

H. C. Kim*, J. Y. Yoo*, H. S. Kang* and S. W. Kim*

(Received May 17, 1995)

An experimental study has been performed in an attempt to seek some possibilities of obtaining the solutions of heat transfer problems related to rotor-stator disk cavity systems of gas turbine engines by analogy with corresponding problems in mass transfer which arises from using naphthalene sublimation technique. Measurements are made to examine the effects of rotational Reynolds number, the flow rate and the gap ratio on the radial pressure distributions. Pressure inversion phenomenon has been verified to exist for the case of shrouded disks with radial clearance, which perform better in terms of heat transfer, too, than those with axial clearance. The stator flow reattachment points are determined directly by the dual sensor pressure probes and compared well with those estimated from the distributions of static pressure and mass transfer coefficients.

Key Words : Rotor- Stator Disk Cavity, Naphthalene Sublimation Technique, Pressure Inversion, Viscous Pumping

Nomenclature

C_w : $\dot{m}/\mu r_0$ = mass flow coefficient
 D : disk diameter
 D_{naph} : diffusion coefficient of the naphthalene
 G : gap ratio (s/r_0)
 G_{ca} : axial clearance ratio (axial clearance/ s)
 G_{cr} : radial clearance ratio (radial clearance/ s)
 h_m : mass transfer coefficient
 \dot{m} : mass flow rate
 P : static pressure
 P_{atm} : atmospheric pressure
 Re_ω : $\omega r_0^2/\nu$ = rotational Reynolds number
 r_0 : disk radius
 s : gap between rotor and stator
 Sh : Sherwood number ($h_m D/D_{\text{naph}}$)
 μ : viscosity
 ν : kinematic viscosity
 ω : angular velocity (rad/s)

of utmost importance in turbomachinery design. In gas turbine engines, for example, detailed knowledge of temperature distribution on the rotor and stator disks is needed to predict thermal stresses and durability. Thus, researches dealing with rotating disks have been performed by many researchers over the past few decades (Owen (1984) and Bunker et al. (1992)).

As far as gas turbine engines are concerned, there are many circumstances where coolant flows are introduced between the rotor disk and stationary housing. This flow serves not only to supply coolant flow to the disk surface, but also to restrict the radial inflow of hot gases to be ingested into the clearance from the turbine blade flow field. Phadke and Owen (1983) studied a variety of rim seals. They observed that some seals with a radial clearance could, unlike axial clearance seals, exhibit a pressure inversion effect so that cavity pressures at the outer radii were seen to increase rather than decrease with rotational speed. Bhavnani et al. (1992) made experimental measurement for the fluid flow in models of gas turbine disk cavities. Experiments were performed on 70cm-diameter disks for rotational Reynolds

1. Introduction

Heat transfer phenomenon in rotating disks are

* Department of Mechanical Engineering, College of Engineering, Seoul National University, Seoul 151-742, Korea

numbers up to 2.29×10^6 . Velocity and pressure distributions were measured and compared with those of previous theoretical and experimental studies for a free rotating disk and an unshrouded plane rotor-stator disk system. Metzger et al. (1991) developed an experimental method that utilizes encapsulated liquid crystals to determine the local heat transfer on a rotating disk in conjunction with a color CCD camera and automated image analysis. Bunker et al. (1992) then applied this method to investigate hub injection of coolant over a wide range of parameters including disk rotational Reynolds numbers of 2 to 5×10^5 , rotor/stator spacing-to-disk radius ratios of 0.025 to 0.15, and jet mass flow rates between 0.10 and 0.40 times the turbulent pumped flow rate of a free rotating disk.

In the present study we are also interested in the rotor and stator disk systems with and without a shroud. However, we pursue the possibility that the well established naphthalene sublimation technique may be applied to determine the local heat transfer in the rotor - stator system by using the analogy between heat and mass transfers.

2. Experimental Apparatus and Methods

Figure 1 shows a schematic of the test apparatus. The rotor and stator disks are made of bakelite and acrylic plastic, respectively, of 35mm thickness and 450mm diameter. The maximum vertical level difference in the rotor disk surface position is $35 \mu\text{m}$ which is measured through a dial indicator by rotating the disk slowly for several revolutions. The stator disk contains 34 static pressure holes of 1mm diameter which are located at intervals of 5mm in the radial direction from $r/r_0=0.24$ to $r/r_0=0.98$. To check the symmetry of the pressure distribution, exactly the same number of static pressure holes are made on the opposite side of the stator disk. The pressure signals are transmitted to the pressure transducer through a scanivalve with 48 ports.

The jet nozzle, which is fixed perpendicularly at the center of the stator disk, uses a circular jet of 62mm diameter. A heat exchanger is installed near the exit of the blower to maintain a constant

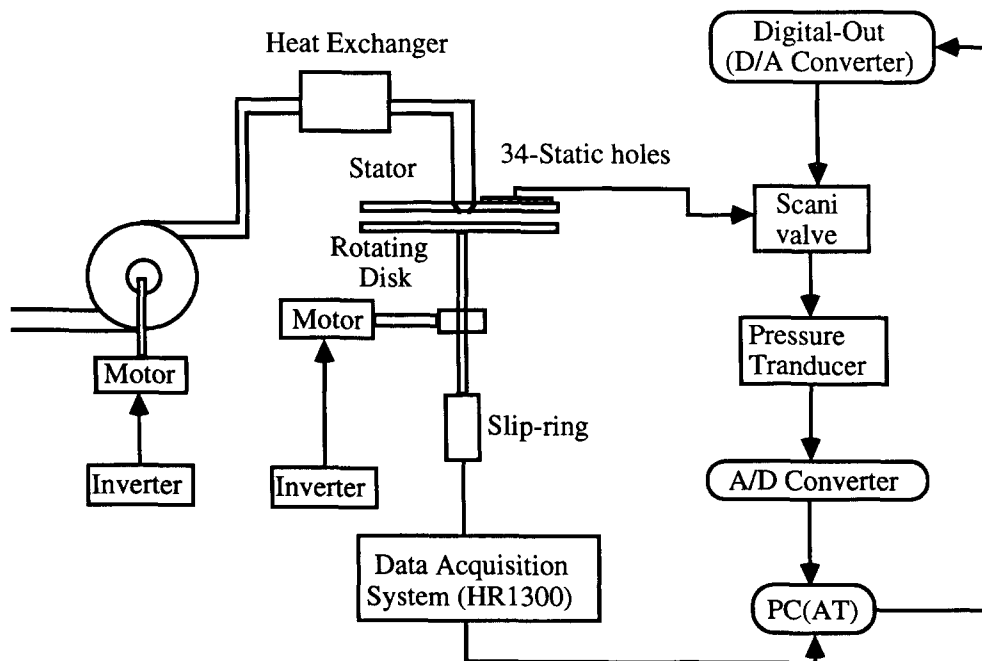


Fig. 1 Schematic of experimental apparatus

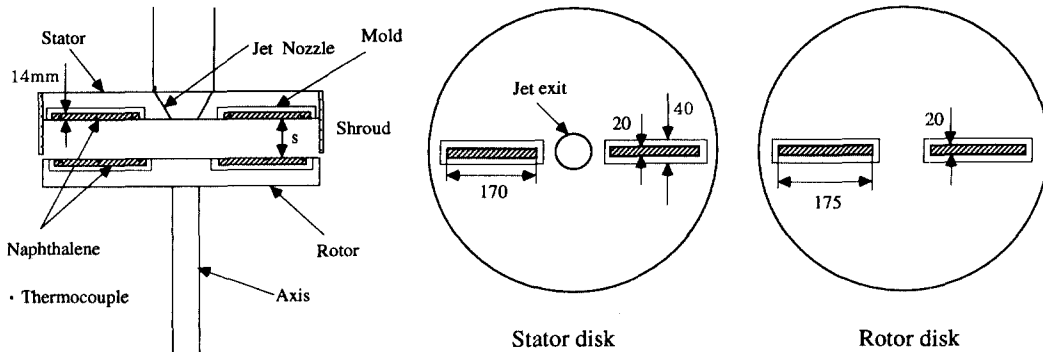


Fig. 2 Schematic of the disk-cavity test section with naphthalene molds

temperature of the air.

Figure 2 shows a schematic of the disk cavity test section with naphthalene molds installed on the rotor and stator disk surfaces, while Fig. 3 shows geometries of axial and radial gaps. The shroud which is made of acrylic plastic of 1.2mm thickness includes an attached rim at the stator disk edge. In order to measure the mass transfer coefficient on disk surfaces, naphthalene molds are installed flush with the surfaces of rotor and stator disks, which are made of duralumin of 180mm length, 40mm width and 14mm depth. On the bottom of each mold, there are three holes through which T-type copper-constantan thermocouples are inserted to check the isothermal condition and 2 bolt-taps with which the naphthalene mold is fixed to the disk. Six thermocouples are installed underneath the naphthalene surfaces of the rotor and stator disks respectively. Another

thermocouple is installed near the exit of the jet nozzle to measure the temperature of the coolant air. The output signal from each thermocouple is transmitted to HR1300 Data Acquisition System. A six channel slip ring assembly is used to receive the output signal from the rotor disk. During each set of experiment, the temperature is maintained at $25 \pm 0.3^\circ\text{C}$ for 90 minutes. The surface elevation of the naphthalene is measured by Linear Variation Differential Transformer (LVDT) with resolutions of $0.1\mu\text{m}$, which is mounted on an X-Y table operated by a step motor controller. Then the local Sherwood number can be obtained by the change in the surface elevation of the naphthalene before and after the test, which is defined as

$$Sh = \frac{h_m \cdot D}{D_{naph}}, \quad (1)$$

where an empirical formula suggested by Goldstein and Cho (1993) is used for the diffusion coefficient of the naphthalene

$$D_{naph} = 8.1771 \times 10^{-7} T^{1.983}. \quad (2)$$

One of the sources of error that may occur in experiments using naphthalene sublimation technique is the loss due to natural convection during the process. To compensate for this error, the amount of sublimated naphthalene under condition at $Re_w=0$, $C_w=0$, and $G=0.10$ for 90 minutes is measured. The percentage of loss due to natural convection measured in this way turns out to be less than 4% of the total loss during each set of rotating experiment for the same period of time. It takes about ten minutes to measure the sublimated naphthalene depth. Thus, the uncer-

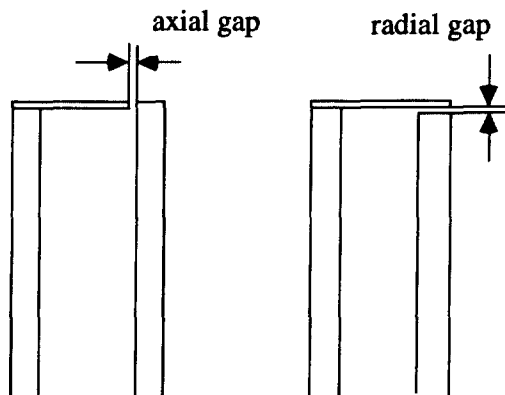


Fig. 3 Geometries of axial and radial gaps

tainty due to natural convection during this measurement is assumed to be within 0.5%, compared with the total loss along the radius. Hence, the results obtained after correcting accordingly the primary measurements of the surface elevation of the naphthalene will be shown in the following section, which accounts for only the forced convection.

Another important factor in the naphthalene sublimation experiment that has to be considered may be the analogy of the boundary conditions. Since in the present study, naphthalene mold surfaces are formed in strips along the radius, there are jumps in the boundary conditions (i.e., constant temperature and adiabatic boundary conditions) across the borders between the disk and the naphthalene surfaces. To examine the extent of error caused by this arrangement, the sublimation depth of the naphthalene is measured in the tangential direction across the mold strip. The results show a maximum deviation of less than 1.5%. In addition, the concentration of naphthalene inside the rotating cavity becomes steady shortly after each set of the experiment commences. Thus it can be deduced that the results will approximate the heat transfer experiment where the entire disk surface is maintained to be adiabatic.

Although the existence of stator flow reattachment has been suggested by some previous studies (Bunker et al., 1992), no attempts were ever made to determine its location directly. In the present study, eight dual sensor pressure probes of 3mm width are installed at radial intervals of 1cm from $r/r_0=0.24$ to $r/r_0=0.53$. To prevent the interference with other probes, they are arranged in the forward-curved formation against the rotational direction of the rotor disk. The stator flow reattachment will then be determined as the location where the difference in the pressure signals sensed along the forward flow and the reverse flow directions becomes zero.

3. Results and Discussion

3.1 Static pressure distribution

Static pressure distributions for the cases of

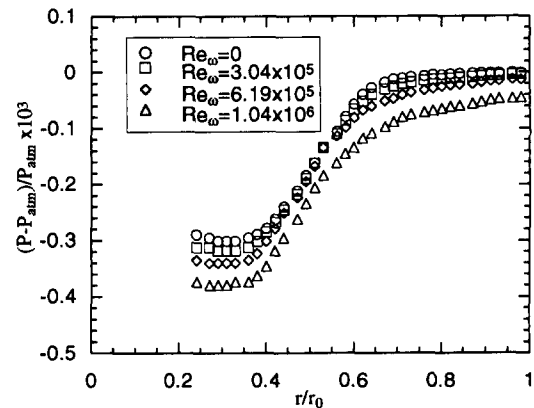


Fig. 4 Effect of Re_ω on radial pressure distribution for unshrouded disks with $C_w=7067$ and $G=0.10$

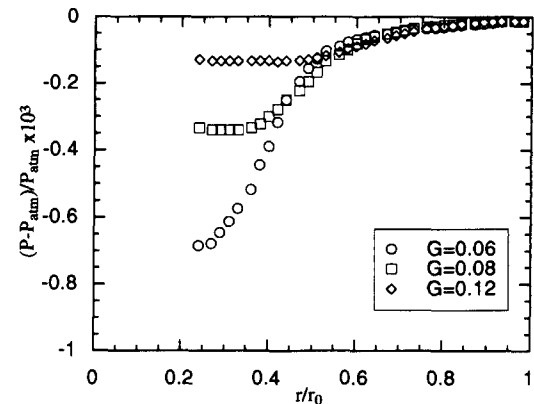


Fig. 5 Effect of G on the radial pressure distribution for unshrouded disks with $Re_\omega=6.19 \times 10^5$ and $C_w=7067$

unshrouded and shrouded disks are measured to confirm the validity of the present study by comparing with previous studies such as Phadke and Owen (1983) and Bhavnani et al. (1992). The error associated with the symmetry of the radial pressure distribution is confirmed to fall within 2%.

In the case of unshrouded disks, the effects of the rotational Reynolds number Re_ω , the flow rate C_w and the gap ratio G on radial pressure distribution have been considered.

Figure 4 shows that for fixed C_w and G , the static pressure decreases as Re_ω increases due to the viscous pumping action. Figure 5 shows that for

fixed Re_ω and C_w , the pressure gradient becomes gentler as G increases. When air is supplied at the centerline to produce a radially outward flow into the cavity between the two disks, the stator pressure distribution altered considerably. This effect is shown in Fig. 6. For fixed Re_ω and G , the pressure gradient becomes steeper as C_w increases due to the increase of radial velocity component in the region from $r/r_0=0.4$ to $r/r_0=0.7$. It can be seen that at large radial locations ($r/r_0=0.7-1.0$) both the pressure gradients and the pressures approach zero. At small radii ($r/r_0<0.4$), the local flow is affected strongly by the throughflow. These suggest that a recirculation zone exists at small radii as indicated qualitatively in Fig. 7 and as discussed earlier by Bhavnani et al. (1992). In fact, Figures 4 to 6 are all in qualitative agreement with them.

In the cases of shrouded disks with axial and

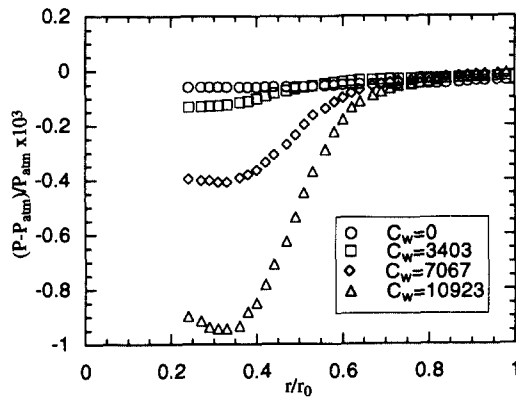


Fig. 6 Effect of C_w on radial pressure distribution for unshrouded disks with $Re_\omega=6.19 \times 10^5$ and $G=0.10$

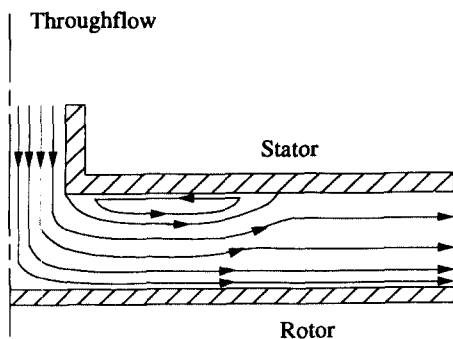
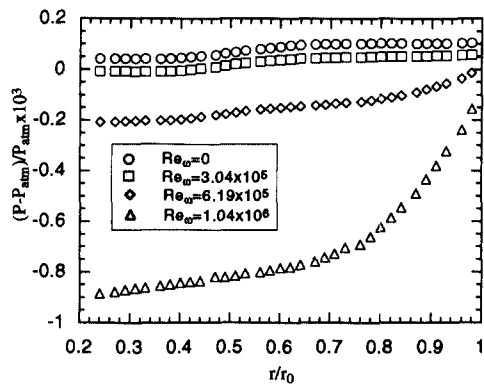


Fig. 7 Qualitative flow pattern for unshrouded disks

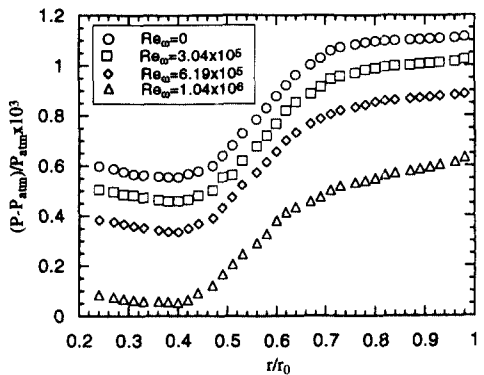
radial clearances, the effects of Re_ω on radial pressure distribution have been considered for three different C_w 's.

Figures 8 (a) and (b) show the experimental results obtained for shrouded disks with axial clearance. The static pressure increases as C_w increases and it decreases as Re_ω increases. From the results obtained for smaller values of C_w , it is noted that for $Re_\omega=1.04 \times 10^6$, there occurs a rapid pressure gradient where $r/r_0>0.7$. This is thought to be due to the predominant effect of disk pumping through which the flow near the stator is sucked toward the rotor side, resulting in a larger radial velocity component.

Figures 9 (a) and (b) show the results obtained for shrouded disks with radial clearance, where the pressure levels at all radii of the stator disk become higher, compared with Figures 8 (a) and (b), respectively. This will prevent a possible



(a) $C_w=3403$



(b) $C_w=10923$

Fig. 8 Effect of Re_ω on radial pressure distribution for shrouded disks with $G_{ca}=0.011$:

radial inflow of hot external gas through the clearance, which is very desirable in sealing the cavity. In particular, in Fig. 9 (b), the pressure-inversion phenomenon (increase of pressure with rotational speed in the case of radial gap) is prominent for all values of r/r_0 , displaying negligible variation in the pressure distribution according to Re_ω , compared with Figs. 8 (a), 8 (b) and 9 (a). This pressure-inversion effect may have occurred due to the following two mechanisms (Phadke and Owen, 1983). First, the large centrifugal force on the rotor surface causes the coolant boundary layer which develops on the rotor surface separate at the disk edge. Then, part of outgoing coolant returns back to the cavity along the shroud (which is much larger than for the case of radial gap). Second, the outer cylindrical surface of the rotor disk will develop a boundary layer when the disk is rotating. Therefore, the

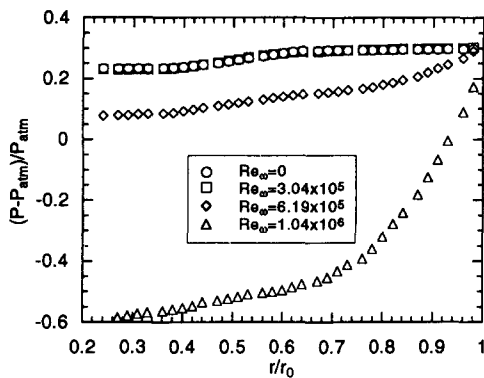
coolant air flow interacts with this rotating cylindrical boundary layer. A combination of the above two mechanisms can result in the observed pressure inversion phenomenon. The results obtained for the static pressure distributions are in good qualitative agreement with Phadke and Owen (1983). It is also noted that the reattachment points are almost fixed at about $r/r_0=0.4$, regardless of Re_ω .

Figure 10 shows the radial pressure distributions on the stator for shrouded disks with $C_w=10923$ and $Re_\omega=1.04 \times 10^6$. And the results are compared with those obtained by Phadke and Owen (1983) under $C_w=11900$ and $Re_\omega=1.0 \times 10^6$. Although the pressure levels are lower than their experimental results due to 8% less C_w and 4% larger Re_ω , the general trends are shown to agree.

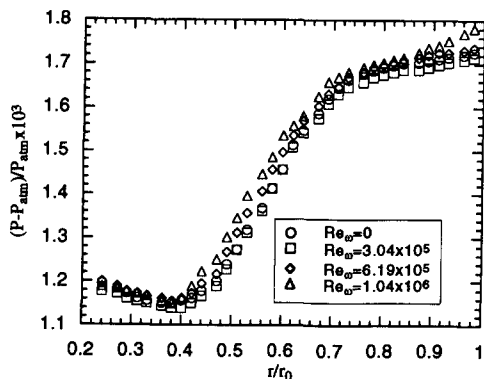
3.2 Mass transfer measurement

In the naphthalene sublimation test, the naphthalene surface is exposed to the flow for 90 minutes before the sublimated depth is measured. The symmetry of the radial distribution of local mass transfer coefficient is confirmed by measuring the sublimation depths of the naphthalene placed at symmetric positions on both the rotor and stator disks. The error falls within 3.5%.

In the case of unshrouded disks, the effects of Re_ω and C_w on the radial distribution of Sh on



(a) $C_w = 3403$



(b) $C_w = 10923$

Fig. 9 Effect of Re_ω on radial pressure distribution for shrouded disks with $G_{cr}=0.011$

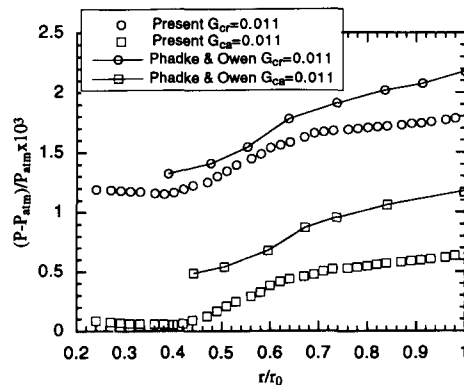


Fig. 10 Radial pressure distributions on the stator for shrouded disks with $C_w=10923$ and $Re_\omega=1.04 \times 10^6$, compared with those obtained by Phadke and Owen (1983) under $C_w=11900$ and $Re_\omega=1.0 \times 10^6$

the rotor disk have been considered, as well as the effects of G on the radial distribution of Sh on the rotor and stator disks, which are not shown here to conserve space. However, it can be said that the stator flow reattachment points correspond to the maximum points of Sh on the stator disk.

Figures 11 and 12 show the effects of Re_ω on radial distribution of Sh on the rotor disks for shrouded disks with axial and radial clearances respectively. The values of Sh obtained for the case with radial clearance are generally higher than those with axial clearance, and at about $r/r_0=0.6\sim 0.7$, there is a division of impinging jet dominated region and rotationally dominated region.

Figures 13 and 14 show the effects of Re_ω on

radial distribution of Sh on the stator disks for shrouded disks with axial and radial clearances respectively. The general trends, particularly, the stator flow reattachment points are nearly the same. At radial locations outside the reattachment, the gradients of Sh appear to be steeper than for unshrouded disks. This is also due to the predominant effect of disk pumping, as mentioned in the previous section.

It is somewhat difficult to directly compare the present results with those obtained previously through heat transfer experiments, because there are differences in experimental conditions and geometries. However, the general trends of the present results are shown to agree qualitatively with Bunker et al. (1992), when we refer to their

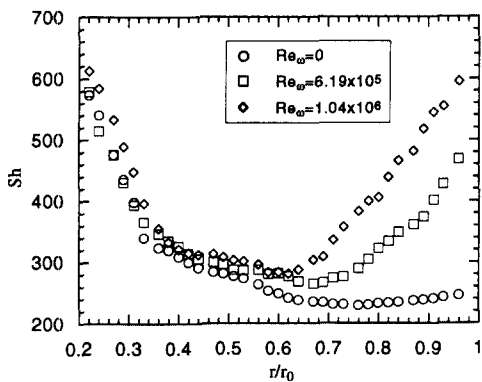


Fig. 11 Effect of Re_ω on radial distribution of local Sherwood number on the rotor for shrouded disks with $C_w=3403$ and $G_{cr}=0.011$.

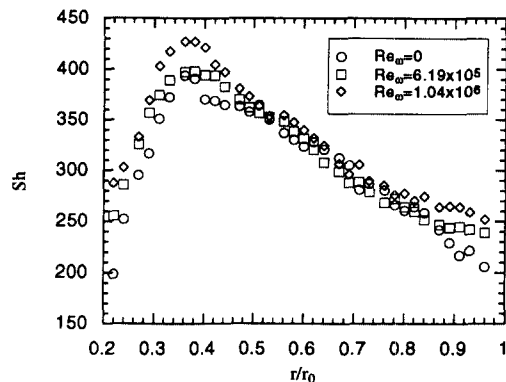


Fig. 13 Effect of Re_ω on radial distribution of local Sherwood number on the stator for shrouded disks with $C_w=3403$ and $G_{cr}=0.011$.

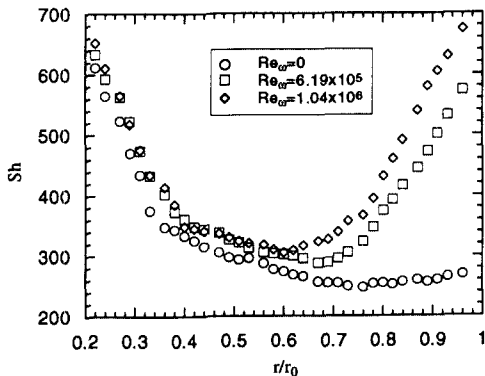


Fig. 12 Effect of Re_ω on radial distribution of local Sherwood number on the rotor for shrouded disks with $C_w=3403$ and $G_{cr}=0.011$.

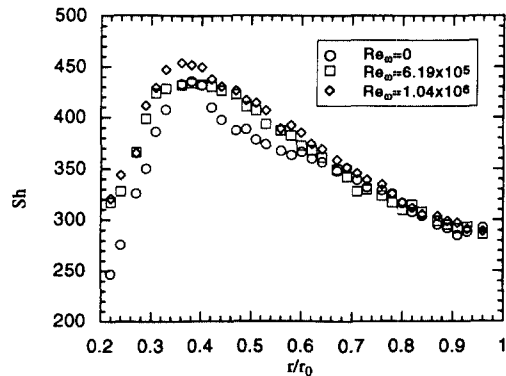


Fig. 14 Effect of Re_ω on radial distribution of local Sherwood number on the stator for shrouded disks with $C_w=3403$ and $G_{cr}=0.011$.

Figs. 9 and 10, above all.

Figure 15 compares the average Sherwood numbers obtained for different shroud arrangements and different rotational Reynolds numbers. In general, mass transfer from the rotor is greater than that from the stator because the convective velocity on the rotor surface is apparently higher than that on the stator surface. It is also noted that mass transfer is more active in the case of shrouded disks with radial clearance than with axial clearance because the sealing effect of the radial clearance is greater. Since the pressure inversion phenomenon increases the mass transfer, the flow in the cavity has a strong mixing effect in the case of shrouded disks with radial clearance.

Figure 16 compares rotor-averaged Nu with Bunker et al. (1992), which is obtained by using

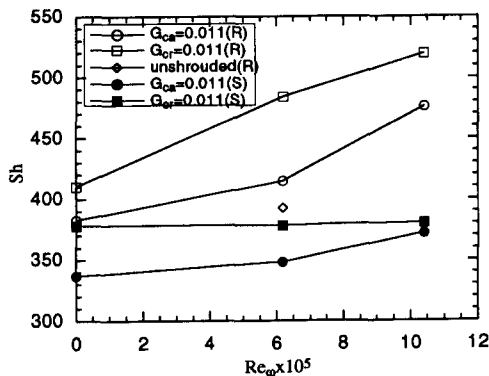


Fig. 15 Distribution of average Sherwood numbers for $C_w = 10923$ and $G = 0.10$.

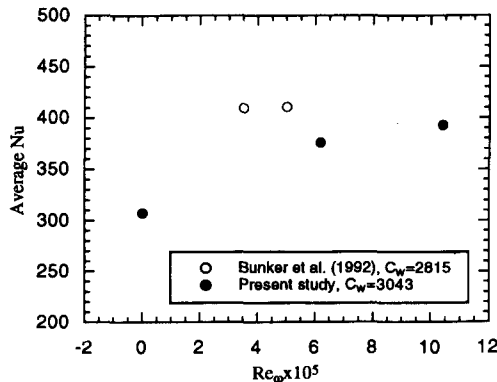


Fig. 16 Comparison of rotor-averaged Nu with Bunker et al. (1992) for $G = 0.10$.

the relation $Nu/Sh = (Pr/Sc)^n$ between Nu in heat transfer system and Sh in mass transfer system under constant temperature boundary condition. The value of n used in the present experiment is $1/3$. Although C_w in the present study is larger than that of Bunker et al. (1992), rotor-averaged Nu falls below their results, which is considered to be due to the difference in the boundary condition and in the shape of the shroud rim surfaces. They used tapered rims, while we used right-angled ones.

3.3 Reattachment point

Figure 17 shows distributions of differences in radial pressures sensed through two pressure holes of dual sensor pressure probes. The reattachment points can be determined as the location where the pressure differences become zero.

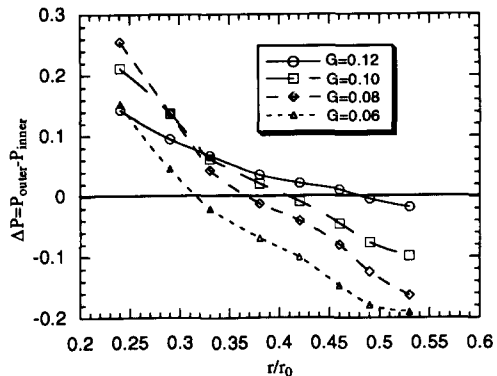


Fig. 17 Radial pressure difference distributions measured by dual sensor pressure probe.

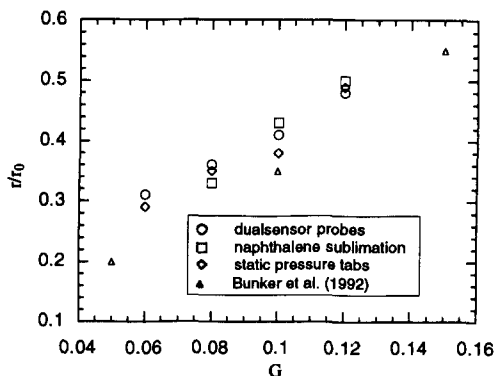


Fig. 18 Comparison of reattachment points on the stator measured by different methods.

In Fig. 18, reattachment points obtained by static pressure measurement, naphthalene sublimation experiment and dual sensor pressure probe measurement are compared, with those predicted by Bunker et al. (1992). The locations of reattachment points are in good qualitative agreement with each other. The present results predict the locations of reattachment points at radial distances slightly larger than those by Bunker et al., again because they used a tapered shroud rim surface and different ratios of jet diameter to disk diameter (0.138 for the present study vs. 0.05 for Bunker et al.). The fact that the maximum heat or mass transfer point is located somewhat upstream of the reattachment point when the flow reattaches after separation can not be confirmed in the present study. Because of the finite volume of dual sensor probe (about 3mm) and the discrete positions of static taps (5mm), we are not able to locate precisely the exact reattachment point.

4. Conclusion

The major conclusions of the present study can be summarized as follows:

(1) Through the measurement of static pressure distributions, it has been shown that the shrouded disks with radial clearance are more effective in preventing the ingress phenomenon than those with axial clearance, for which pressure inversion phenomenon is found to exist.

(2) As far as the mass transfer is concerned, the shrouded disks with radial clearance also perform better than those with axial clearance.

(3) The location of stator flow reattachment point is understood to be where the pressure gradient suddenly increases and the mass transfer coefficient becomes maximum, which agrees with the location where the pressure difference between the two pressure holes of the dual sensor pressure probe becomes zero. And the location of the reattachment point is largely affected by the gap size between stator and rotor rather than rotational Reynolds number, Re_ω and mass flow coefficient, C_w .

Acknowledgement

The authors wish to acknowledge the support for this work by the Turbo and Power Machinery Research Center.

References

- Bayley, F. J. and Owen, J. M., 1970, "The Fluid Dynamics of a Shrouded Disk System with a Radial Outflow of Coolant," *ASME Journal of Engineering for Power*, 92, 335~341.
- Bhavnani, S. H., Khodadadi, J. M., Goodling, J. S. and Waggott, J., 1992, "An Experimental Study of Fluid Flow in Disk Cavities," *ASME Journal of Turbomachinery*, Vol. 114, pp. 454~461.
- Bunker, R. S., Metzger, D. E. and Wittig, S., 1992, "Local Heat Transfer in Turbine Disk Cavities: Part I - Rotor and Stator Cooling with Hub Injection of Coolant," *ASME Journal of Turbomachinery*, Vol. 114, pp. 211~220.
- Goldstein, R. J. and Cho, H. H., 1993, "A Review of Mass (Heat) Transfer Measurements Using Naphthalene Sublimation," *Proceedings of the 3rd World Conference on Experimental Heat Transfer, Fluid Mechanics and Thermodynamics*, Hawaii.
- Haynes, C. M. and Owen, J. M., 1975, "Heat Transfer from a Shrouded Disk System with a Radial Outflow of Coolant," *ASME Journal of Engineering for Power*, Vol. 110, pp. 78~85.
- Metzger, D. E., Bunker, R. S. and Bosch, G., 1991, "Transient Liquid Crystal Measurement of Local Heat Transfer on a Rotating Disk with Jet Impingement," *ASME Journal of Turbomachinery*, Vol. 113, pp. 52~59.
- Mochizuki, S., 1993, "Unsteady Flow Phenomena and Heat Transfer in Rotating-Disk Systems," *Proceedings of the 6th International Symposium on Transport Phenomena in Thermal Engineering*, Vol. 3, pp. 279~289.
- Owen, J. M., 1984, "Fluid Flow and Heat Transfer in Rotating Disk Systems, Heat and Mass Transfer in Rotating Machinery," eds.,

Metzger, D. E. and Afgan, N. H., Hemisphere, Washington, DC.

Phadke, U. P. and Owen, J. M., 1983, "An Investigation of Ingress for an 'Air-Cooled'

Shrouded Rotating Disk System with Radial-Clearance Seals," *ASME Journal of Engineering for Power*, Vol. 105, pp. 178~183.